Predictive Modeling and Parameter Optimization of Cutting Forces During Orbital Drilling

Shan Yicai (单以才)[1,2*], *Li Liang* (李亮)[2], *He Ning* (何宁)[2], *Qin Xiaojie* (秦晓杰)[2], *Zhang Ting* (章婷)[3]

1. Nanjing College of Information Technology, Nanjing, 210046, P. R. China;
2. College of Mechanical and Electrical Engineering, Nanjing University of Aeronautics and Astronautics, Nanjing, 210016, P. R. China;
3. School of Mechanical Engineering, Nanjing Institute of Technology, Nanjing, 211167, P. R. China

(Received 22 October 2013; revised 16 March 2014; accepted 30 March 2014)

Abstract: To optimize cutting control parameters and provide scientific evidence for controlling cutting forces, cutting force modeling and cutting control parameter optimization are researched with one tool adopted to orbital drill holes in aluminum alloy 6061. Firstly, four cutting control parameters(tool rotation speed, tool revolution speed, axial feeding pitch and tool revolution radius) and affecting cutting forces are identified after orbital drilling kinematics analysis. Secondly, hybrid level orthogonal experiment method is utilized in modeling experiment. By nonlinear regression analysis, two quadratic prediction models for axial and radial forces are established, where the above four control parameters are used as input variables. Then, model accuracy and cutting control parameters are analyzed. Upon axial and radial forces models, two optimal combinations of cutting control parameters are obtained for processing a ∅13 mm hole, corresponding to the minimum axial force and the radial force respectively. Finally, each optimal combination is applied in verification experiment. The verification experiment results of cutting force are in good agreement with prediction model, which confirms accracy of the research method in practical production.

Key words: orbital drilling; cutting force; hybrid level orthogonal experiment method; prediction model; parameter optimization

CLC number: TG146.23 **Document code**: A **Article ID**: 1005-1120(2014)05-0521-09

1 Introduction

With the widely use of titanium alloy, carbon fiber reinforced plastics(CFRP) and aluminum alloy in aviation parts, highly efficient and precise hole-making technology has become a research hotspot[1-2]. As a new hole-making technology, orbital drilling has some advantages including small axial force, minor tool wear, convenient chip removal, high dimension accuracy, etc. And compared with conventional drilling, it can process various holes with one tool. Therefore, orbital drilling has a broad application prospect in aviation assembly[3-5].

As radial and axial cutting edges both participate in cutting, it is more difficult to control cutting forces in orbital drilling than in conventional drilling. Research on cutting forces and parameter optimization of orbital drilling has great values on machining accuracy enhancement and processing quality improvement. By now, many scholars have conducted various experimental and theoretical researches on cutting forces of orbital drilling.

On the aspect of theoretical modeling, Bayoumi, et al. analyzed the relation between cutting

Foundation items: Supported by the National Natural Science Foundation of China (50975141); the Aviation Science Fund (20091652018, 2010352005); the National Science and Technology Major Project of the Ministry of Science and Technology of China (2012ZX04003031-4).

* **Corresponding author**: Shan Yicai, Associate Professor, E-mail: nj_syc@163.com.

parameters and tool rotation angle, then established an analytic model of cutting forces. Further, the effect of radial and axial engagements and cutting speed on the cutting parameters was investigated[6]. Qin Xuda, et al. simplified the influence of cutting forces on axial cutting edge into a z-direction single force, then presented a novel analytical model of cutting force[7]. Under certain time domain, Liu Changyi established cutting force models with inputs as helical feeding, spindle rotation speed, axial and radial cutting depth and tool geometric parameters[8]. As orbital drilling process is effected by various factors (impact load, tool wear, chip deformation, etc.), large deviation is inevitable between theoretical and measured cutting forces.

On the aspect of experimental studies, Ni Wangyang analyzed orbital drilling kinetics, and investigated the influence of revolution speed, axial feeding rate and revolution radius on cutting forces[9]. Iyer et al. carried out contrast experiments between orbital drilling and conventional drilling on die steel AISI D2. The research confirmed the superiority of orbital drilling in the aspects of cutting forces, hole quality and tool wear, ect[10]. Denkena, et al. analyzed the impact of axial and tangential feed on milling forces through undeformed chip model[11]. Hiroyuki Sasahara studied the effect of minimum quantity lubrication on chip temperature, chip deformation, cutting temperature, cutting forces and shape error, and finally pointed out that the cutting force of orbital drilling was smaller than that of conventional drilling[12]. Wang Ben pointed out that there was little difference between x-direction cutting force in orbital drilling and that in conventional drilling, while z-direction cutting force in orbital drilling was smaller than that in conventional drilling[13]. Though the influence of cutting parameters on cutting forces has been analyzed, prediction model of cutting force has not been established in above references.

In China, Yuan Zhixing built up cutting force models of x- and z-direction through orbital drilling in die steel. These models neglected the effect of revolution radius on cutting forces[14]. Wang Haiyan, et al. built a multi-objective optimization model with two objectives including tool life and material removal rate. Pareto genetic algorithm was introduced to optimize cutting parameters[15].

If conventional cutting parameters are used as inputs in establishing cutting force models of orbital drilling, forces of axial and radial edges need to be built respectively. We attempt to avoid the complexity of modeling with two edges, and chose four cutting control parameters as inputs. To realize predicting and controlling cutting forces during orbital drilling, we focus on establishing models of cutting forces when machining different holes with one tool, and optimizing cutting control parameters.

2 Kinematics Analysis of Orbital Drilling

Fig. 1 shows the principle of orbital drilling[16]. During orbital drilling, tool practises three movements simultaneously (rotation around own axis, feed along axial direction, and revolution around hole axis). Several control parameters should be considered as the following:

Hole diameter: D

Tool diameter: d

Axial feeding pitch: P

Tool rotation speed: n_s

Tool revolution speed: n_ω

Tool revolution radius: e

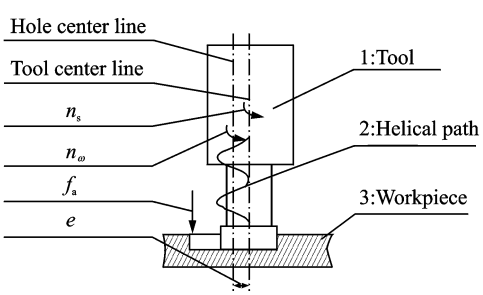

Fig. 1 Schematic diagram of orbital drilling

Axial feeding pitch P represents the axial feeding after tool finishes revolution for a round. Hence, tool axial feed speed f_a can be expressed as

$$f_a = P * n_\omega \tag{1}$$

Tool revolution radius e is the radial offset of tool axis from hole axis. In revolution, tangential feed speed f_t of tool center point (TCP) is

$$f_t = (2\pi * e) * n_\omega \tag{2}$$

As tool screw feed is composed of axial and tangential feeds, screw feed speed f_C of TCP is

$$f_C = \sqrt{(P * n_\omega)^2 + (2\pi * e * n_\omega)^2} \tag{3}$$

If tool tooth number is Z, the TCP cutting amount per tooth δ_C can be described as

$$\delta_C = \frac{f_C}{n_s * Z} = \sqrt{\left(\frac{P * n_\omega}{n_s * Z}\right)^2 + \left(\frac{2\pi * e * n_\omega}{n_s * Z}\right)^2} = \sqrt{(f_{za})^2 + (f_{zt})^2} \tag{4}$$

where f_{za} and f_{zt} are tool feeding per tooth in axial and tangential directions.

During orbital drilling, tool tangential cutting amount per tooth δ_P is different from δ_C. It is expressed as

$$\delta_P = \delta_C * (D/(D-d)) \tag{5}$$

As we all know, the cutting amount per tooth is directly related to cutting forces. The more cutting amount per tooth is, the bigger the resistance to overcome in chip formation is. Thus, Macro milling force is increased. From Eqs. (1—5), we know that cutting forces of orbital drilling can be determined by control parameters as n_s, n_ω, P, e, d, D and Z. As for a special tool, the influence of tool geometric parameters on cutting forces can be eliminated.

3 Experimental Design

3.1 Experimental conditions

Orbital drilling experiment is conducted on Mikron UCP710 high speed machining center, as shown in Fig. 2. In the center, spindle power is 16 kW and spindle speed is 100—18 000 r/min. The workpiece material is aluminum alloy 6061. The workpiece size is 200 mm × 100 mm × 15 mm. The tool is H602411-10 from German Walter company, which has 45° helix angle and two teeth. Dry cutting and inverse milling are adopted in the experiment. Cutting force measurement system is composed of Kistler 9265B dynamic force measurement instrument, Kistler 5019 charge amplifier, and computer data acquisition subsystem.

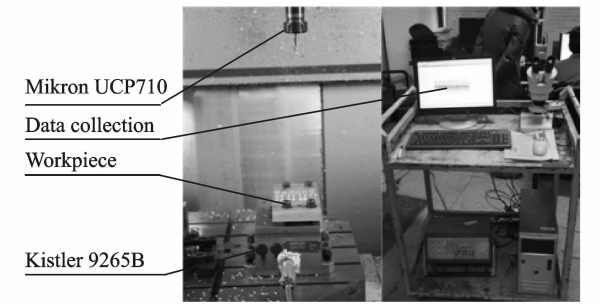

Fig. 2 Experimental setup for milling forces measurement

3.2 Experimental scheme

Under specific machine tool and cutting tool, the main parameters affecting cutting forces are tool rotation speed, axial feeding pitch, tool revolution speed and tool revolution radius. For different materials and workpieces, a lot of experiments should be done for analyzing the influence of cutting parameters on cutting forces. To reduce experimental cost, orthogonal experiment method is utilized in experimental design[17]. In actual production, variation of n_s leads to different axial cutting depth. Oversized revolution radius degrades machinability of orbital drilling. Hence, there is no need to use too many levels in tool axial feeding pitch and tool revolution radius. With reference to the different hole diameters and the hole processing security in aviation components, experimental factors and levels are designed as Table 1.

Table 1 Cutting control parameters and levels

Parameters	Factor levels			
n_s/(r · min^{-1})	3 000	4 000	5 000	6 000
n_ω/(r · min^{-1})	15.92	23.87	31.82	
P/mm	1	2		
e/mm	1	2		

4 Model Establishment and Accuracy Analysis

4.1 Characteristic analysis on cutting forces in orbital drilling

As influenced by radial and axial cutting edges in processing, the cutting force of orbital drilling is obviously different from that in conven-

tional drilling[18]. Fig. 3(a) shows the waveform graph of milling force in x-direction, which is composed by one low frequency signal and one high frequency signal. The low frequency waveform is caused by tool revolution, while the high frequency waveform is mainly determined by tool rotation. The high frequency is also influenced by high speed vibration and various disturbances. Two types of waveform graph are shown in Figs. 3(b,c).

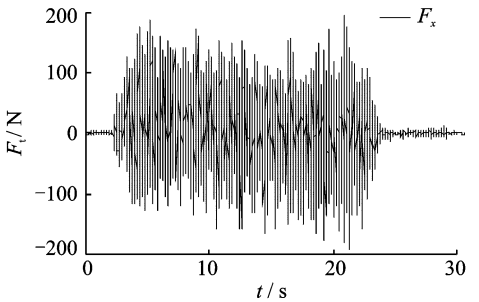

(a) Waveform figure of milling force

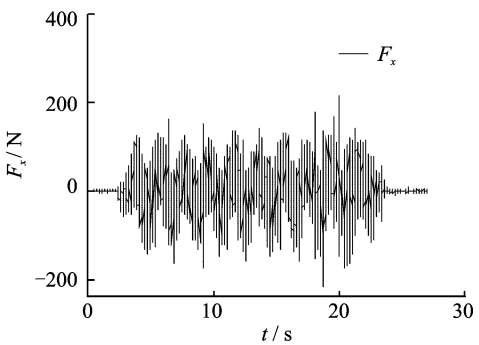

(b) Low frequency waveform graph

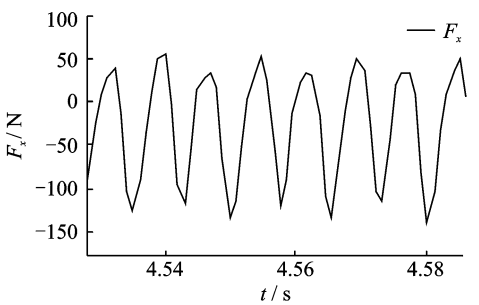

(c) High frequency waveform graph

Fig. 3 Waveform graph of cutting force in x-direction

Cutting force measurement system can detect three milling forces as F_x, F_y and F_z simultaneously. In workpiece reference coordinate system, the three forces compose the cutting resultant force of orbital drilling. If tool coordinate system is set as a reference, the cutting resultant force can also be decomposed into tangential force F_t, radial force F_r, and axial force F_a. Here, F_r is the main factor affecting hole dimensional error and shape precision. F_a causes quality defects as burr of metal material and delamination of CFRP. F_t is mainly used to calculate consumed power. Therefore, the research on cutting force in tool coordinate system is significant for improving machining accuracy[19]. According to Fig. 2, cutting component forces in tool coordinate system can be calculated as

$$\begin{cases} F_t = F_x \cdot \sin(2\pi n_\omega t) - F_y \cdot \cos(2\pi n_\omega t) \\ F_r = F_x \cdot \cos(2\pi n_\omega t) + F_y \cdot \sin(2\pi n_\omega t) \\ F_a = F_z \end{cases} \quad (6)$$

To avoid calculation error caused by low frequency signal, we utilize high frequency waveform to calculate measured value of cutting force. Under signal stable stage, we select 100 adjacent peaks and troughs. A bigger peak and a bigger trough are selected respectively from each four adjacent peaks and troughs. Then, the average values of peak and trough are calculated respectively. The bigger absolute average value is regarded as measured value of cutting force. We attempt to study axial and radial forces for further improving hole quality by controlling cutting forces and optimizing cutting parameters in orbital drilling. In experiment, various combinations of four cutting control parameters are designed and the values of F_r and F_a are measured. The values are shown as Table 2.

Table 2 Cutting control parameters and cutting forces in experiment

Test No.	n_s / (r·min^{-1})	n_ω / (r·min^{-1})	P / mm	E / mm	F_r / N	F_a / N
1	3 000	15.92	1	1	51.16	59.27
2	3 000	31.82	1	1	56.05	100.92
3	3 000	23.87	2	2	124.51	119.34
4	3 000	31.82	2	2	134.43	145.07
5	4 000	15.92	2	1	56.81	107.96
6	4 000	31.82	2	1	77.62	144.18
7	4 000	23.87	1	2	81.32	107.82
8	4 000	31.82	1	2	85.96	112.58
9	5 000	15.92	1	1	55.55	78.51
10	5 000	31.82	1	1	63.38	95.57
11	5 000	23.87	2	2	174.40	119.23
12	5 000	31.82	2	2	206.85	140.82
13	6 000	15.92	2	1	38.77	89.38
14	6 000	31.82	2	1	57.12	108.81
15	6 000	23.87	1	2	53.20	97.41
16	6 000	31.82	1	2	60.60	92.29

4.2 Establishment of prediction model

According to Table 2, models of F_r and F_a are built and the influence of cutting control parameters on cutting forces is studied. Since there is different dimension and boundary in cutting control parameters, the four parameters need to be normalized, where linear function conversion is used as

$$y_i = \frac{x_i - x_{\min}}{x_{\max} - x_{\min}} \quad i = 1, 2, 3, 4 \tag{7}$$

where x reflects the original value, y the converted value, $x_{\min}$ and $x_{\max}$ are the minimum and the maximum of x.

After normalization process, the data conversion is shown as Table 3.

After data normalization, prediction models of F_r and F_a are established by four cutting control parameters. To overcome the shortcoming of direct-vision method in distinguishing conditional error from accidental error , variance analysis is introduced in the research. The established models are described as Eqs. (8a,8b).

Table 3 Results of data normalization

y_1	y_2	y_3	y_4	$y_1 * y_2$	$y_1 * y_3$	$y_1 * y_4$	$y_2 * y_3$	$y_2 * y_4$	$y_3 * y_4$	$y_1 * y_1$	$y_2 * y_2$	$y_3 * y_3$	$y_4 * y_4$	F_r	F_a
0.000 0	0.0	0	0	0.000 0	0.000 0	0.000 0	0.0	0.0	0	0.000 0	0.00	0.0	0	0.073 7	0.000 0
0.000 0	1.0	0	0	0.000 0	0.000 0	0.000 0	0.0	0.0	0	0.000 0	1.00	0.0	0	0.102 8	0.485 4
0.000 0	0.5	1	1	0.000 0	0.000 0	0.000 0	0.5	0.5	1	0.000 0	0.25	1.0	1	0.510 1	0.700 1
0.000 0	1.0	1	1	0.000 0	0.000 0	0.000 0	1.0	1.0	1	0.000 0	1.00	1.0	1	0.569 1	1.000 0
0.333 3	0.0	1	0	0.000 0	0.333 3	0.000 0	0.0	0.0	0	0.111 1	0.00	1.0	0	0.107 3	0.567 5
0.333 3	1.0	1	0	0.333 3	0.333 3	0.000 0	1.0	0.0	0	0.111 1	1.00	1.0	0	0.231 1	0.989 6
0.333 3	0.5	0	1	0.166 7	0.000 0	0.333 3	0.0	0.5	0	0.111 1	0.25	0.0	1	0.253 2	0.565 9
0.333 3	1.0	0	1	0.333 3	0.000 0	0.333 3	0.0	1.0	0	0.111 1	1.00	0.0	1	0.280 8	0.621 3
0.666 7	0.0	0	0	0.000 0	0.000 0	0.000 0	0.0	0.0	0	0.444 4	0.00	0.0	0	0.099 8	0.224 2
0.666 7	1.0	0	0	0.666 7	0.000 0	0.000 0	0.0	0.0	0	0.444 4	1.00	0.0	0	0.146 4	0.423 1
0.666 7	0.5	1	1	0.333 3	0.666 7	0.666 7	0.5	0.5	1	0.444 4	0.25	1.0	1	0.806 9	0.698 8
0.666 7	1.0	1	1	0.666 7	0.666 7	0.666 7	1.0	1.0	1	0.444 4	1.00	1.0	1	1.000 0	0.950 5
1.000 0	0.0	1	0	0.000 0	1.000 0	0.000 0	0.0	0.0	0	1.000 0	0.00	1.0	0	0.000 0	0.350 9
1.000 0	1.0	1	0	1.000 0	1.000 0	0.000 0	1.0	0.0	0	1.000 0	1.00	1.0	0	0.109 2	0.577 4
1.000 0	0.5	0	1	0.500 0	0.000 0	1.000 0	0.0	0.5	0	1.000 0	0.25	0.0	1	0.085 9	0.444 5
1.000 0	1.0	0	1	1.000 0	0.000 0	1.000 0	0.0	1.0	0	1.000 0	1.00	0.0	1	0.129 9	0.384 8

$$\begin{aligned} F'_a = {} & 0.018\ 3 + 0.738 * y_1 + 0.499 * y_2 + \\ & 0.398 * y_3 + 0.167 * y_4 - 0.410 * y_1 * y_2 - \\ & 0.81 * y_1 * y_3 + 0.124 * y_1 * y_4 + \\ & 0.179 * y_2 * y_3 - 0.059\ 6 * y_2 * y_4 - \\ & 0.159 * y_3 * y_4 - 0.617 * y_1 * y_1 \end{aligned} \tag{8a}$$

$$\begin{aligned} F'_r = {} & 0.078\ 3 + 0.547 * y_1 + 0.019\ 9 * y_2 - \\ & 0.161 * y_3 - 0.062\ 4 * y_4 + 0.019\ 3 * y_1 * \\ & y_2 + 0.28 * y_1 * y_3 + 0.209 * y_1 * y_4 + \\ & 0.095\ 1 * y_2 * y_3 + 0.084\ 7 * y_2 * y_4 + \\ & 0.535 * y_3 * y_4 - 0.757 * y_1 * y_1 \end{aligned} \tag{8b}$$

Next, reverse normalized processing is made by Eqs. (8a,8b), the relationships are calculated between n_s , n_ω , P, e, and F_a (or F_r), multiple quadratic regression models are gained as follows

$$\begin{aligned} F_a = {} & -186 + 6.98 * 10^{-2} * x_1 + 3.99 * x_2 + \\ & 48 * x_3 + 23.4 * x_4 - 7.38 * 10^{-4} * x_1 * x_2 - \\ & 5.19 * 10^{-3} * x_1 * x_3 + 3.65 * 10^{-3} * x_1 * \\ & x_4 + 0.966 * x_2 * x_3 - 0.321 * x_2 * x_4 - \\ & 13.7 * x_3 * x_4 - 6 * 10^{-6} x_1^2 \end{aligned} \tag{9a}$$

$$\begin{aligned} F_r = {} & 72.8 + 8.7 * 10^{-2} * x_1 - 1.89 * x_2 - 180 * \\ & x_3 - 150 * x_4 - 6.8 * 10^{-5} * x_1 * x_2 + \\ & 1.57 * 10^{-2} * x_1 * x_3 + 1.17 * 10^{-2} * x_1 * \\ & x_4 + 1.01 * x_2 * x_3 + 0.895 * x_2 * x_4 + \\ & 90 * x_3 * x_4 - 1.4 * 10^{-5} * x_1^2 \end{aligned} \tag{9b}$$

where the four input values as x_1, x_2, x_3 and x_4 correspond to n_s, n_ω , P and e, respectively. According to the four input values in Table 2, fitted values of F_r and F_a can be worked out through Eqs. (9a,9b).

The point is that (9a,9b) can only be used when parameters meet certain demands

$$\begin{cases} 3\ 000\ \text{r/min} \leqslant n_s \leqslant 6\ 000\ \text{r/min} \\ 15.92\ \text{r/min} \leqslant n_\omega \leqslant 31.82\ \text{r/min} \\ 1\ \text{mm} \leqslant P \leqslant 2\ \text{mm} \\ 1\ \text{mm} \leqslant e \leqslant 2\ \text{mm} \end{cases} \tag{10}$$

4.3 Accuracy analysis of prediction models

In variance analysis, F criterion is introduced in significance testing. The results are shown in Table 4.

Table 4 Adequacy of prediction models

Force	Source of variation	D_F	S_S	MS	F	$F_{1-0.05}$	R^2	Adjusted R^2
F_r	Regression	11	1.251 9	0.113 8	81.16	5.96	0.996	0.983
	Error	4	0.005 6	0.001 4				
	Total	15	1.257 5					
F_a	Regression	11	1.099 4	0.099 9	31.58	5.96	0.989	0.957
	Error	4	0.012 7	0.003 2				
	Total	15	1.112 1					

In Table 4, D_F is a degree of freedom, S_S is sum of squares, MS is mean square, and R^2 is determination coefficient.

Under given significant level α, regression model is credible if $F < F_{1-0.05}(p, n-p-1)$. From Table 4, the F values of the two models are both less than $F_{1-0.05}$. Eqs. (8a, 9a) have high significance when $\alpha=0.05$. R^2 of F_r and F_a models are 0.996 and 0.989. The adjusted R^2 are 0.983 and 0.957. These indicate that the predicted values of F_r and F_a are consistent with experimental values(as shown in Fig. 4). The analysis shows that the models are fit for predicting cutting forces of orbital drilling in aluminium alloy 6061.

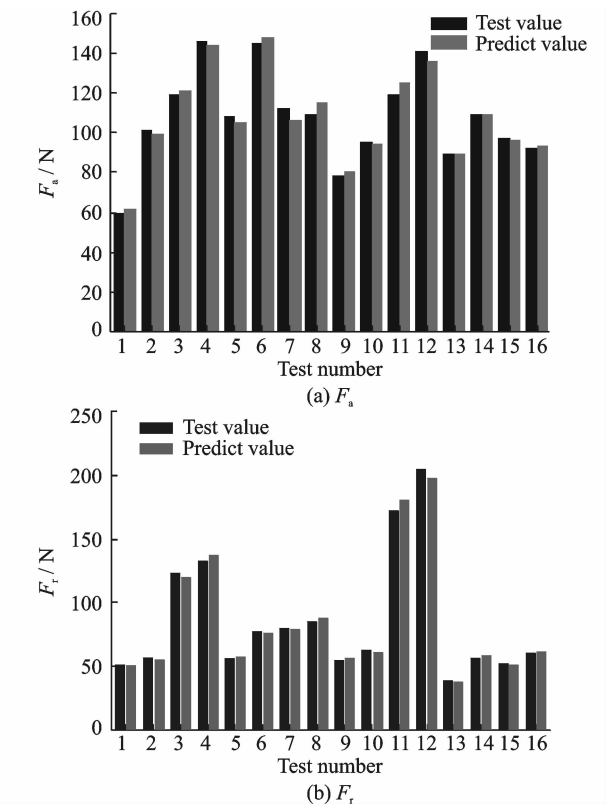

Fig. 4 Comparison of predictive value with test value

5 Effect of Cutting Control Parameters on Cutting Forces

In regression model, when three input parameters are fixed at a certain level, the model will become a single-factor model. When P and e are both set as 1mm, the relationship curves between F_a (or F_r) and n_ω are shown in Fig. 5, where n_ω is set as 15.92, 23.87, 31.82 r/min respectively. With the increase of n_s, F_a and F_r increase at first but decrease finally. In the low-speed stage, tool tooth friction is predominant. The increase of n_s causes the increase of F_a and F_r. In high-speed stage, f_{za} and f_{zt} decrease with the increase of n_s. Consequently, F_a and F_r decrease accordingly. In this stage, tool feeding becomes the main factor to determine milling force. Fig. 5(a) indicates that F_a increases with the increase of n_ω. Fig. 5(b) gives the relationship between n_ω and F_r. Obviously, the three curves are similar under three tool revolution speeds.

When P and e are both 1 mm and n_s is set as 3 000, 4 500, 6 000 r/min, respectively, the relationship curves of F_a (or F_r) and n_ω are shown in Fig. 6. F_a and F_r increase with the increase of n_ω. As can be seen from Eq. (4), the increase of n_ω enlarges the values of f_{za} and f_{zt}. Fig. 6(a) shows that the influence of n_ω on F_a is obvious when n_s is low. But the influence becomes small with n_s increasing. In Fig. 6(b), the increase of n_ω has little influence on F_r.

When n_ω is 15.92 r/min, e is 1 mm, and n_s is

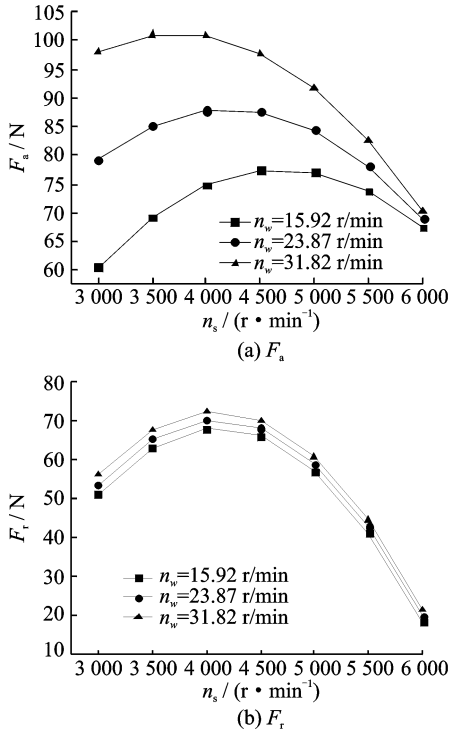

Fig. 5 Effect of n_s on F_a and F_r

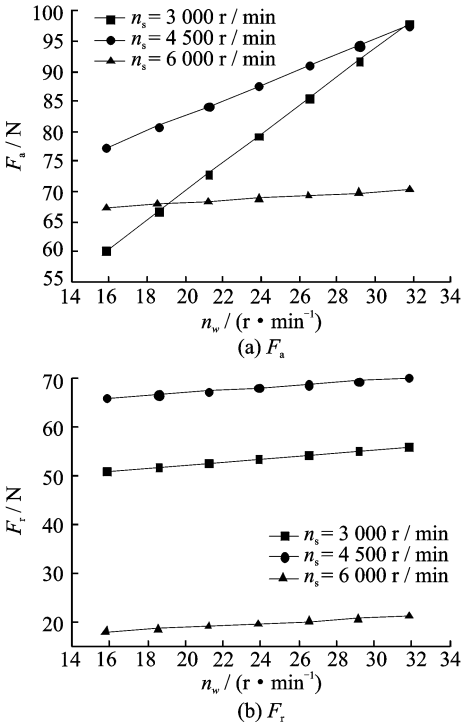

Fig. 6 Effect of n_ω =15.92 r/min on F_a and F_r

3 000, 4 500, 6 000 r/min, the relation curves of F_a (or F_r) and P are shown in Fig. 7. As for radial cutting edge, axial cutting depth f_{za} increases with P. And, f_{zt} of axial cutting edge also enlarges. Consequently, F_a increases significantly under the special n_s, which can be seen from Fig. 7

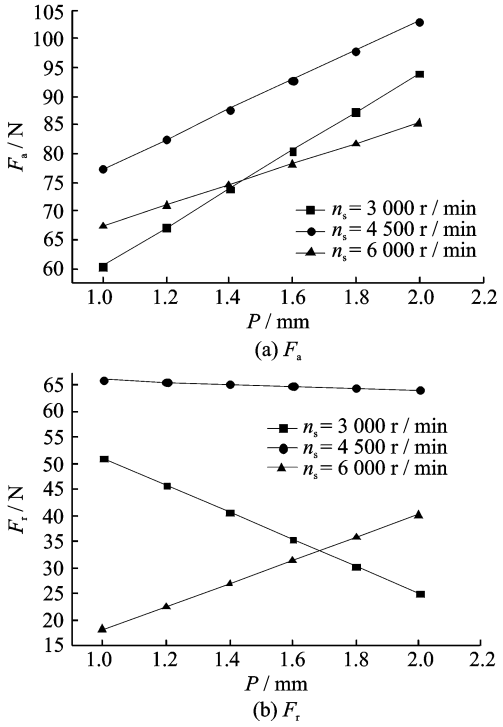

Fig. 7 Effect of P on F_a and F_r

(a). In low-stage, F_a increases with the increase of n_s. But, F_a decreases with the sharp increase of n_s. In low n_s of Fig. 7(b), F_r decreases with the increase of P. The reason is that under selected tool and certain revolution radius, the increase of P amplifies cutting effect similar to conventional drilling. But F_r increases under high rotation speed. The reason is that the sharp increase of n_s produces cutting effect more similar to milling. In this case, n_s has greater influence on F_r than P.

We set the following parameters: P=1 mm, n_s =3 000, 4 500, 6 000 r/min. In Fig. 8(a), the increase of e enlarges f_{zt} under the special n_s, and further increases F_a. In low n_s, the fluence of the tool-workpiece friction on cutting forces is predominant in orbital drilling, which leads to the increase of F_a. In high n_s, the sharp decrease of f_{zt} and f_{za} causes the decrease of F_a. Under low n_s, the increase of e reduces F_a as shown in Fig. 8 (b). The reason is that the tool-workpiece space for chip removal is increased and the materials removal cut by radial cutting edge is multiplied. While in high n_s, tool dynamic characteristic exerts greater influence on cutting forces, where F_r increases accordingly.

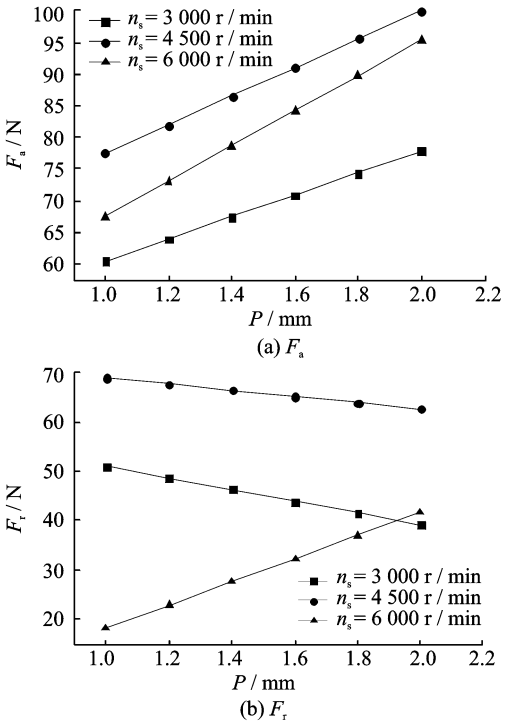

Fig. 8 Effect of e on F_a and F_r

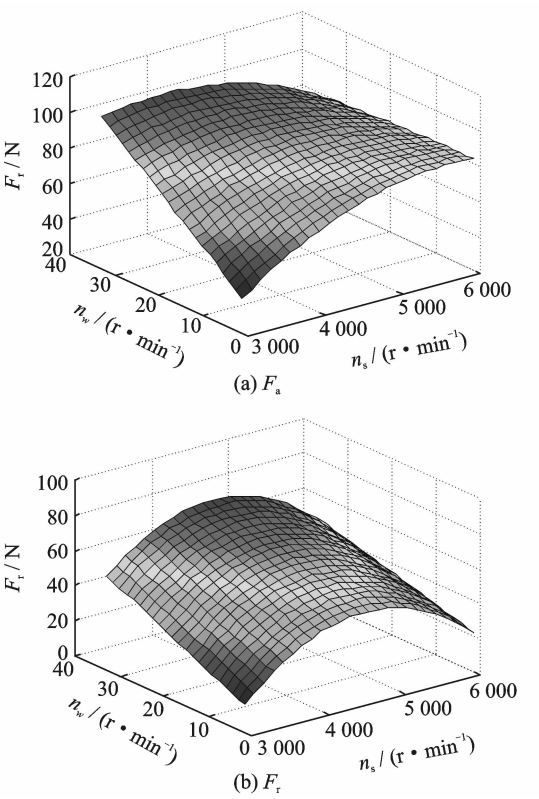

Fig. 9 Response surface of milling forces based on prediction model

6 Optimization of Cutting Control Parameters

To process a ∅13 hole in aluminum alloy 6061, we choose tool H602411-10. If $P=1$ mm, response surfaces of F_a and F_r based on prediction models are shown in Fig. 9.

To achieve the minimum value of F_a (or F_r), we need to optimize combination of n_s, n_ω, and P. The optimization method should satisfy the given objective function

$$F_i(x)=F_i(n_s,n_\omega,P,e,)\rightarrow \min F_i(x) \quad (11)$$

where $i=$ a, r (Note: a means axial, r means radial).

To achieve machining efficiency, the processing time of the hole is set as 30 s. The constraints of cutting control parameters are

$$\begin{cases} 3\ 000\ \text{r/min} \leqslant n_s \leqslant 6\ 000\ \text{r/min} \\ 15.92\ \text{r/min} \leqslant n_\omega \leqslant 31.82\ \text{r/min} \\ 1\ \text{mm} \leqslant P \leqslant 2\ \text{mm} \\ n_\omega \times P = 30\ \text{s} \end{cases} \quad (12)$$

As the objective function is multivariate nonlinear equation, it is uneasy to find a combination of optimal cutting control parameters through analytic method or experimental method. To solve the problem, we combined penalty function method with prediction models to optimize cutting control parameters.

After multiple iterative solutions of objective functions, two optimum combinations are worked out as

$$x_a^* = (n_s^*, n_\omega^*, P^*) = (4\ 189, 25.3, 1.2),$$

$$x_r^* = (n_s^*, n_\omega^*, P^*) = (4\ 367.5, 30, 1)$$

Under two combinations as x_a^* and x_r^*, theoretical and experimental values of F_a and F_r are obtained. The results are:

Theoretical values: $F_a = 103.99$ N, $F_r = 83.73$ N.

Experimental values: $F_a = 108.68$ N, $F_r = 85.49$ N.

The consistency between theoretical and experimental values indicates that the optimization method is feasible and practicable in cutting control parameter optimization of orbital drilling. In practical application, the optimization of F_r can be used to improve hole dimensional error and shape precision. If burr at hole export needs to be strictly controlled in special occasion, the optimization of F_a can be selected.

7 Conclusions

(1) Upon analyzing orbital drilling kinematics, main cutting control parameters are determined as n_s, n_ω, P and e, which impose great effect on cutting forces when processing with one selected tool. Nonlinear regression analysis is introduced in prediction models of F_a and F_r, in which four milling control parameters are used as inputs. By F criterion, the F values are 81.16 and 31.58, which show good significance of two cutting force models. Meanwhile, the determination coefficients R^2 of 0.996 and 0.989 prove the high fitting precision of the models.

(2) The influence of cutting control forces on F_a and F_r has been studied based upon prediction models. With the increase of n_s, F_a and F_r increase firstly and then decrease. The increase of n_ω can increase F_a and F_r. When P and e both increase, F_a increases accordingly, while F_r increases first and then decreases.

(3) Under selected scope of cutting control parameters, Matlab software is used to optimize cutting control parameters with the optimization goals as minimum F_a and F_r. Comparison between theoretical analysis and verification experiment shows that the prediction errors of F_a and F_r are both less than 5%, which proves the validity of the cutting force model during orbital drilling. But how to realize the collaborative optimization of F_a and F_r will be our major research direction in future.

References:

[1] Jiang Chengyu, Wang Junbiao. Key manufacturing technologies of large aircraft development in China [J]. Aeronautical Manufacturing Technology, 2009 (1):28-31. (in Chinese)

[2] Bo Yong, Xu Guokang, Xiao Qingdong. Automatic precision drilling technology of aircraft structural part [J]. Aeronautical Manufacturing Technology, 2009(24): 61-64. (in Chinese)

[3] Whinnem E. Development and deployment of orbital drilling at Boeing[C]// Aerospace Manufacturing and Automated Fastening Conference and Exhibition. USA: SAE, 2006: 2006-01-3152.

[4] Whinnem E, Lipczynski G, Eriksson I. Development of orbital drilling for the Boeing 787 [J]. SAE Int J Aerosp, 2009, 1(1):811-816.

[5] Marguet B, Wiegert F, Lebahar O, et al. Advanced portable orbital drilling unit for airbus final assembly lines [C]// Aerospace Technology Conference and Exposition. USA: SAE, 2007: 2007-01-3849.

[6] Bayoumi A E, Yucesan G, Kendall L A. An analytic mechanistic cutting force model for milling operations: a case study of helical milling operation [J]. Transactions of the ASME, 1994, 8 (114):331-339.

[7] Wang Haiyan, Qin Xuda, Ren Chengzu, et al. Prediction of cutting forces in helical milling process [J]. Int Adv Manuf Tchnol, 2011, 58(9/10/11/12):849-859.

[8] Liu Changyi, Wang Gui, Dargusch M S. Modelling, simulation and experimental investigation of cutting forces during helical milling operations [J]. Int Adv Manuf Tchnol, 2012,63(9/10/11/12):839-850.

[9] Ni Wangyang. Orbital drilling of aerospace materials [C]// SAE 2007 Transactions Set. Los Angeles: SAE International, 2008(V116): 2007-01-3814.

[10] Iyer R, Koshy p, Eg E. Helical milling: an enabling technology for hard machining holes in AISI D2 tool steel[J]. Int J Mach Tool Manuf, 2007, 47 (2):205-210.

[11] Denkena B, Boehnke D, Dege J H. Helical milling of CFRP-titanium layer compounds [J]. CIRP Journal of Manufacturing Science and Technology, 2008, 2 (1): 64-69.

[12] Sasahara H, Kawasaki M, Tsetsumi M. Helical feed milling with MQL for boring of aluminum alloy [J]. Trans Jpn Soc Mech Eng C, 2003, 69(8): 2156-2161.

[13] Wang Beng, Gao Hang, Bi Mingzhi, et al. Mechanism of reduction of damage during orbital drilling od C/E composites [J]. Journal of mechanical engineering, 2012, 48(15):173-181.

[14] Yuan Zhixing. Dynamics research on helical milling [D]. Tianjing: School of Mechanical Engineering, Tianjing University, 2008.

[15] Wang Haiyan, Qin Xuda, Ren Chengzu, Optimization of cutting parameters in helical milling process based on pareto genetic algorithm [J]. China Mechanical Engineering, 2012, 23(17): 2058-2061.

[16] Brinkmeier E, Fangmann S, Meyer I. Orbital drilling kinematics [J]. Annals of the WGP Production Engineering, 2008, 2(3): 277-284.

[17] Zhang Runchu, Liu Minqian, Yang Jianfeng, et al. Statistics for experimenters design, innovation, and discovery[M]. Beijing: China Machine Press, 2010. (in Chinese)

[18] Shan Yicai, He Ning, Li Liang, et al. Orbital milling hole of aerospace al-alloy with big pitch. Transactions of Tianjin University [J]. 2011, 17(5): 229-235.

[19] Geng Guosheng. Fundamental research on high speed milling of titanium alloys [D]. Nanjing: Nanjing University of Aeronautics and Astronautics, 2006.

(Executive editor: Zhang Bei)